Design of an efficient terahertz source using triply resonant nonlinear photonic crystal cavities

Design of an efficient terahertz source using triply resonant nonlinear photonic crystal cavities

Ian B. Burgess[1†], Yinan Zhang[1†], Murray W. McCutcheon[1†], Alejandro W. Rodriguez[2], Jorge Bravo-Abad[2], Steven G. Johnson[3], Marko Lončar[1*]

[1] *School of Engineering and Applied Sciences, Harvard University, Cambridge, MA 02138*

[2] *Department of Physics, Massachusetts Institute of Technology, Cambridge, MA, 02139*

[3] *Department of Mathematics, Massachusetts Institute of Technology, Cambridge, MA, 02139*

† *These authors contributed equally.*

loncar@seas.harvard.edu

Abstract: We propose a scheme for efficient cavity-enhanced nonlinear THz generation via difference-frequency generation (DFG) processes using a *triply* resonant system based on photonic crystal cavities. We show that high nonlinear overlap can be achieved by coupling a THz cavity to a doubly-resonant, dual-polarization near-infrared (e.g. telecom band) photonic-crystal nanobeam cavity, allowing the mixing of three mutually orthogonal fundamental cavity modes through a $\chi^{(2)}$ nonlinearity. We demonstrate through coupled-mode theory that complete depletion of the pump frequency – i.e., quantum-limited conversion – is possible. We show that the output power at the point of optimal total conversion efficiency is adjustable by varying the mode quality (Q) factors.

OCIS codes: (190.4223) Nonlinear wave mixing; (230.4320) Nonlinear optical devices; (190.4975) Parametric processes.

References and links

1. R.W. Boyd, *Nonlinear Optics* (Academic Press, 2003).
2. M.A. Belkin, F. Capasso, A. Belyanin, D.L. Sivco, A.Y. Cho, D.C. Oakley, C.J. Vineis, G.W. Turner, "Terahertz quantum-cascade-laser source based on intracavity difference-frequency generation," Nature Photonics **1**, 288-292 (2007).
3. M. Bieler, "THz generation from resonant excitation of semiconductor nanostructures: Investigation of second-order nonlinear optical effects," IEEE J. Sel. Top. Quantum Electron. **14**, 458-469 (2008).
4. A. Andronico, J. Claudon, J.M Gerard, V. Berger, G. Leo, "Integrated terahertz source based on three-wave mixing of whispering-gallery modes," Opt. Lett. **33**, 2416-2418 (2008).
5. K. L. Vodopyanov, M.M. Fejer, X. Yu, J.S. Harris, Y.S. Lee, W.C. Hurlbut, V.G. Kozlov, D. Bliss, C. Lynch, "Terahertz-wave generation in quasi-phase-matched GaAs," Appl. Phys. Lett. **89**, 141119 (2006).
6. G. Imeshev, M.E. Fermann, K.L. Vodopyanov, M.M. Fejer, X. Yu, J.S. Harris, D. Bliss, C. Lynch, "High-power source of THz radiation based on orientation-patterned GaAs pumped by a fiber laser," Opt. Express **14**, 4439-4444 (2006).
7. J. Hebling, A.G. Stepanov, G. Almassi, B. Bartal, J. Kuhl, "Tunable THz pulse generation by optical rectification of ultrashort laser pulses with tilted pulse fronts," Appl. Phys. B **78**, 593-599 (2004).
8. M.C. Beard, G.M. Turner, and C.A. Schmuttenmaer, "Terahertz Spectroscopy," J. Phys. Chem. B **106**, 7146-7159 (2002).

#115294 - $15.00 USD Received 4 Aug 2009; revised 15 Oct 2009; accepted 19 Oct 2009; published 20 Oct 2009

9. M. van Exter, D.R. Grischkowsky, "Characterization of an Optoelectronic Terahertz Beam System," IEEE Trans. Microwave Theory Tech. **38**, 1684-1691 (1990).
10. Q. Wu, M. Litz, X.C. Zhang, "Broadband detection capability of ZnTe electro-optic field detectors," Appl. Phys. Lett **68**, 2924-2926 (1996).
11. Y.S. Lee, T. Meade, V. Perlin, H. Winful, T.B. Norris, A. Galvanauskas, "Generation of narrow-band terahertz radiation via optical rectification of femtosecond pulses in periodically poled lithium niobate," Appl. Phys. Lett. **76**, 2505-2507 (2000).
12. J.E. Schaar, K.L. Vodopyanov, M.M. Fejer, "Intracavity terahertz-wave generation in a synchronously pumped optical parametric oscillator using quasi-phase-matched GaAs," Opt. Lett. **32**, 1284-1286 (2007).
13. R. Kohler, A. Tredicucci, F. Beltram, H.E. Beere, E.H. Linfield, A.G. Davies, D.A. Ritchie, R.C. Iotti, F. Rossi,"Terahertz semiconductor-heterostructure laser" Nature **417**, 156-159 (2002).
14. B.S. Williams, S. Kumar, Q. Hu, J.L. Reno, "Operation of terahertz quantum-cascade lasers at 164 K in pulsed mode and at 117 K in continuous-wave mode," Opt. Express **13**, 3331-3339 (2005).
15. M.A. Belkin, J.A. Fan, S. Hormoz, F. Capasso, S.P. Khanna, M. Lachab, A.G. Davies, E.H. Linfield, "Terahertz quantum cascade lasers with copper metal-metal waveguides operating up to 178 K" Opt. Express **16**, 3242-3248 (2008).
16. M.W. McCutcheon, J.F. Young, G.W. Reiger, D. Dalacu, S. Frederick, P.J. Poole, R.L. Williams "Experimental demonstration of second-order processes in photonic crystal microcavities at submilliwatt excitation powers," Phys. Rev. B **76**, 245104 (2007).
17. R.E. Hamam, M. Ibanescu, E.J. Reed, P. Bernel, S.G. Johnson, E. Ippen, J.D. Joannopoulos, M. Soljačić, "Purcell effect in nonlinear photonic structures: A coupled mode theory analysis," Opt. Express **16**, 12523-12537 (2008).
18. M. Soljačić, J.D. Joannopoulos, "Enhancement of nonlinear effects using photonic crystals," Nature Materials **3**, 211-219 (2004).
19. Y.H. Avetisyan, "Cavity-enhanced terahertz region difference-frequency generation in surface-emitting geometry," Proc. SPIE **3795**, 501.
20. M.W. McCutcheon, G.W. Rieger, I.W. Cheung, J.F. Young, D. Dalacu, S. Frederick, P.J. Poole, G.C. Aers, R.L. Williams, "Resonant scattering and second-harmonic spectroscopy of planar photonic crystal microcavities," Appl. Phys. Lett. **87**, 221110 (2005).
21. J. Bravo-Abad, A. Rodriguez, P. Bernel, S.G. Johnson, J.D. Joannopoulos, M. Soljačić, "Enhanced nonlinear optics in photonic-crystal microcavities," Opt. Express **15**, 16161-16176 (2007).
22. A.B. Matsko, D.V. Strekalov, N. Yu, "Sensitivity of terahertz photonic receivers," Phys. Rev. A. **77**, 043812 (2008).
23. A. Rodriguez, M. Soljačić, J.D. Joannopoulos, S.G. Johnson, "$\chi^{(2)}$ and $\chi^{(3)}$ harmonic generation at a critical power in inhomogeneous doubly resonant cavities," Opt. Express **15**, 7303-7318 (2007).
24. I.B. Burgess, A.W. Rodriguez, M.W. McCutcheon, J. Bravo-Abad, Y. Zhang, S.G. Johnson, M. Lončar "Difference-frequency generation with quantum-limited efficiency in triply-resonant nonlinear cavities," Opt. Express **17**, 9241-9251 (2009).
25. H. Hashemi, A.W. Rodriguez, J.D. Joannopoulos, M. Soljačić, S.G. Johnson, "Nonlinear harmonic generation and devices in doubly-resonant Kerr cavities," Phys. Rev. A **79**, 013812 (2009).
26. At the position of highest THz field that exists above the THz material, the field amplitude has $\sim 25\%$ of the maximum field amplitude for our THz nanobeam design.
27. S. Singh, *Nonlinear Optical Materials* in M.J. Weber Ed., *Handbook of laser science and technology, Vol. III: Optical Materials, Part I*, (CRC Press 1986).
28. Y. Zhang, M.W. McCutcheon, I.B. Burgess, M. Lončar, "Ultra-high-Q TE/TM dual-polarized photonic crystal nanocavities," Opt. Lett. **34**, 2694-2696 (2009).
29. M.W. McCutcheon, D.E. Chang, Y. Zhang, M.D. Lukin, M. Lončar, "Broad-band spectral control of single photon sources using a nonlinear photonic crystal cavity," arXiv:0903.4706 (2009).
30. M.W. McCutcheon, M. Lončar, "Design of a silicon nitride photonic crystal nanocavity with a Quality factor of one million for coupling to a diamond nanocrystal" Opt. Express **16**, 19136-19145 (2008).
31. P.B. Deotare, M.W. McCutcheon, I.W. Frank, M.M. Khan, M. Lončar, "High Quality factor photonic crystal nanobeam cavities" Appl. Phys. Lett. **94**, 121106 (2009).
32. Y. Zhang, M. Lončar, "Ultra-high quality factor optical resonators based on semiconductor nanowires" Opt. Express **16**, 17400 (2008).
33. M. Notomi, E. Kuramochi, H. Taniyama, "Ultrahigh-Q Nanocavity with 1D Photonic Gap" Opt. Express **16**, 11095-11102 (2008).
34. R. Herrmann, T. Sunner, T. Hein, A. Loffler, M. Kamp, A. Forchel, "Ultrahigh-quality photonic crystal cavity in GaAs," Opt. Lett. **31**, 1229-1231 (2006).
35. S. Combrie, A. De Rossi, Q.V. Tran, H. Benisty, "GaAs photonic crystal cavity with ultrahigh Q: microwatt nonlinearity at 1.55μm," Opt. Lett. **33**, 1908-1910 (2008).
36. E. Weidner, S. Combrie, N.-V.-Q, Tran, A. De Rossi, J. Nagle, S. Cassete, A. Talneau, H. Benisty, "Achievement of ultrahigh quality factors in GaAs photonic crystal membrane nanocavity," Appl. Phys. Lett. **89**, 221104 (2006).
37. N. Jukam, C. Yee, M.S. Sherwin, I. Fushman, J. Vučković, "Patterned femtosecond laser excitation of terahertz

#115294 - $15.00 USD Received 4 Aug 2009; revised 15 Oct 2009; accepted 19 Oct 2009; published 20 Oct 2009

leaky modes in GaAs photonic crystals," Appl. Phys. Lett. **89**, 241112 (2006)
38. N. Jukam, M.S. Sherwin, "Two-dimensional terahertz photonic crystals fabricated by deep reactive ion etching in Si," Appl. Phys. Lett. **83**, 21-23 (2003).
39. D.X. Qu, D. Grischkowsky, W.L. Zhang, "Terahertz transmission properties of thin, subwavelength metallic hole arrays," Opt. Lett. **29**, 896-898 (2004).
40. Z.P. Jian, J. Pearce, D.M. Mittleman, "Terahertz transmission properties of thin, subwavelength metallic hole arrays," Opt. Lett. **29**, 2067-2069 (2004).
41. C.M. Yee, M.S. Sherwin, "High-Q terahertz microcavities in silicon photonic crystal slabs," Appl. Phys. Lett. **94**, 154104 (2009).
42. H. Kitahara, N. Tsumura, H. Kondo, M.W. Takeda, J.W. Haus, Z.Y. Yuan, N. Kawai, K. Sakoda, K. Inoue, "Terahertz wave dispersion in two-dimensional photonic crystals," Phys. Rev. B **64**, 045202 (2001).
43. K. Srinivasan, P.E. Barclay, M. Borselli, O. Painter, "Optical-fiber-based measurement of an ultrasmall volume high-Q photonic crystal microcavity," Phys. Rev. B **70**, 081306 (2004).
44. A. Taflove, S.C. Hagness, *Computational Electrodynamics: The Finite-Difference Time-Domain Method* (Artech House, 2005).
45. The NIR cavity was included in the THz cavity simulations and it was found to cause a slight decrease in the scattering-limited Q factor ($2 \times 10^6 \rightarrow 1.4 \times 10^6$), while having a negligible effect on κ_T.
46. The effective usable area where the NIR cavity can be fabricated is given by the product of the spacing between the two central holes and the width of the THz cavity.
47. J.D. Joannopoulos, S.G. Johnson, J.N. Winn, R.D. Meade, *Photonic Crystals: Molding the Flow of Light* (Princeton University Press, 2008).
48. K.L. Vodopyanov, Yu.H. Avetisyan, "Optical terahertz wave generation in a planar GaAs waveguide," Opt. Lett. **33**, 2314-2316 (2008).

1. Introduction

Nonlinear optical frequency conversion is widely used for the generation of light in parts of the spectrum for which there are no convenient sources [1]. In particular, nonlinear processes are regarded as a promising route to generation of coherent radiation in the terahertz (THz) frequency range [2–7]. Traditionally, THz radiation [8] has been generated in one of two ways: with a photoconductive antenna [9], or optical rectification (OR) of amplified femtosecond pulses in ZnTe crystals [10]. These techniques have the inherent disadvantage of requiring an ultrafast laser system with high peak powers and bulk, macroscopic optics. The OR approach has subsequently been improved by using quasi-phase-matched $LiNbO_3$ [11] and GaAs [5,12] crystals to increase the nonlinear interaction between the pump and generated signals, and this has yielded an impressive photon conversion efficiency of 3.3% [5]. Recently, there has been renewed interest in cavity-enhanced nonlinear frequency conversion as a means to produce THz radiation. A THz quantum-cascade-laser (QCL) source operating at 80 K, based on the intra-cavity difference-frequency generation (DFG) of two mid-infrared modes [2] has been developed capable of producing 60 nW of power at 60 μm. QCLs that directly emit in the THz are have also been demonstrated with operating temperatures up to 178 K [13–15].

In this work, we are motivated by the recent work on wavelength-scale nonlinear cavities which points towards the possibility of highly efficient nonlinear frequency conversion at low powers on an integrated platform [2–4,16–20]. By virtue of operating at the scale of a single wavelength, the complexities of phase-matching in a propagating-wave system are simplified to simply optimizing the overlap of the cavity modes [21–25], and high photon conversion efficiencies are the result of the long interaction times afforded by high-Q cavities. We propose a scheme for efficient THz generation based on second-order $\chi^{(2)}$ difference frequency process in a triply resonant structure consisting of two nested photonic-crystal cavities, as shown schematically in Fig. 1. The first cavity, designed to operate at near-infrared (NIR) wavelengths and realized in a nonlinear material (e.g. III–V semiconductors), produces nonlinear-polarization at THz frequencies by difference-frequency generation (DFG). The cavity is placed in the proximity of a second, much larger, single-mode cavity with the resonance in the THz range. We utilize the fact that the THz wavelength, λ_T ($\sim 150\mu$m), is on a vastly different length scale

#115294 - $15.00 USD Received 4 Aug 2009; revised 15 Oct 2009; accepted 19 Oct 2009; published 20 Oct 2009

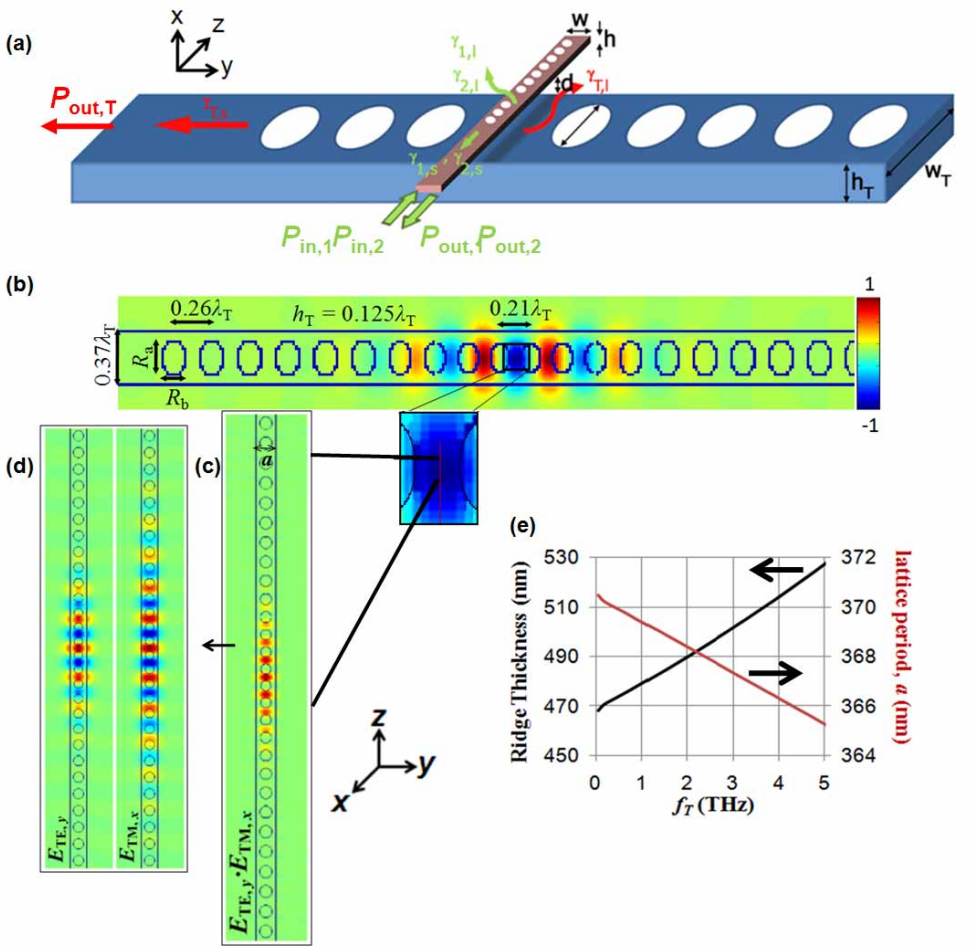

Fig. 1. **(a)** Schematic (not to scale) of the triply resonant system of coupled photonic crystal nanobeam cavities for efficient THz generation. A dual-mode NIR cavity is suspended just above the THz cavity near its field maximum. NIR pump and idler waves are coupled into the cavity via a waveguide extending from one end of the NIR cavity. The THz output is also collected via waveguide coupling. **(b)** Normalized mode profile ($E_{z,\mathrm{T}}$) of the THz mode. **(c)** Diagram of the NIR dual-mode cavity, showing the spatial profile of the nonlinear mode-product ($E_{y,\mathrm{TE}}E_{x,\mathrm{TM}}$, right). The beam width is equal to the lattice period (a) and the spacing of the two central holes is $0.84a$. **(d)** TE- and TM-like mode profiles of the NIR cavity. **(e)**: Nanobeam thickness (black) and lattice period, a, (red) for the NIR PhCNC plotted as a function of the THz difference frequency. The TE-like mode frequency is fixed at 200THz ($\lambda_{\mathrm{TE}} = 1.5\mu\mathrm{m}$, $\lambda_{\mathrm{TE}} < \lambda_{\mathrm{TM}}$).

from the pump and idler wavelengths, λ_1 and λ_2 respectively ($\sim 1.5\mu$m), allowing us to effectively decouple the cavity designs. Our system can be viewed as a classical version of a two-level atom strongly coupled to the optical cavity.

In our design, we suspend the telecom band cavity above the THz cavity near the field maximum [26], sufficiently far so that the telecom modes are not affected by the presence of the THz cavity, but sufficiently close that the long-wavelength THz mode extends substantially into this cavity (e.g. 1μm above). In this way we can achieve a high overlap between the three *funda-*

#115294 - $15.00 USD Received 4 Aug 2009; revised 15 Oct 2009; accepted 19 Oct 2009; published 20 Oct 2009

mental cavity modes by mixing three mutually orthogonal polarizations through the strong $\chi^{(2)}_{ijk}$ ($i \neq j \neq k$) terms in the nonlinear susceptibility of III–V semiconductors (e.g. GaAs, GaP) [16, 27]. This scheme takes advantage of our recently demonstrated doubly-resonant ultrahigh-Q photonic-crystal nanobeam cavities (PhCNC) with mutually orthogonally polarized modes (i.e. one is TE-like one is TM-like) [28, 29]. Each cavity is preferentially over-coupled to a waveguide extending from one end, with the length of the Bragg mirror of holes at that end used to tune the strength of the coupling. The mirror at the other end is made sufficiently long such that leakage in that direction is much smaller than out-of-plane losses. The NIR pump waves are input and the THz output wave is collected via these waveguide modes, as shown schematically in Fig. 1a. Since the relevant nonlinear material is in the NIR cavity, the THz cavity can be composed of any material, a useful degree of freedom considering the scarcity of low-loss THz materials.

2. Model

We employ the coupled-mode theory (CMT) framework described in Ref. [24] to analyze triply resonant THz generation by DFG in a wavelength-scale cavity with a non-resonant $\chi^{(2)}$ nonlinear susceptibility. Our cavity has three resonant modes at frequencies ω_1 (pump), ω_2 (idler), and ω_T (THz signal), which satisfy $\omega_T = \omega_1 - \omega_2$ and each mode is coupled to a waveguide. As described in Ref. [24], the conversion efficiency of the system is determined by the following parameters: the input powers, (P_1, P_2); the cavity mode quality factors Q_k ($k = 1, 2, T$); the cavity waveguide coupling strengths Γ_k, defined as $\Gamma_k \equiv \gamma_{k,s}/(\gamma_{k,s} + \gamma_{k,l})$, where $\gamma_{k,s}$ is the leakage rate into the waveguide and $\gamma_{k,l}$ is the leakage rate due to linear material absorption and scattering (fabrication errors, impurities, mode-mismatches etc.); and the nonlinear coupling constant β, defined in Ref. [24]. As discussed in Ref. [23], avoiding mode symmetries and polarizations that lead to zero coupling constant, as well as optimizing the value of β, is analogous to phase-matching in the nonlinear mixing of propagating modes. For our type of design, since the THz field strength is nearly constant across the much smaller NIR cavity, β is well approximated by:

$$\beta \approx \frac{\kappa_T d_{\text{eff}}}{2\sqrt{\varepsilon_0 \lambda_T^3}} \frac{\int_d d^3\mathbf{r} E^*_{\text{TE},y} E_{\text{TM},x}}{\sqrt{\int d^3\mathbf{r} \varepsilon_r |\mathbf{E}_{\text{TE}}|^2} \sqrt{\int d^3\mathbf{r} \varepsilon_r |\mathbf{E}_{\text{TM}}|^2}}, \tag{1}$$

where $\mathbf{E}_{\text{TE}}$, $\mathbf{E}_{\text{TM}}$, and $\mathbf{E}_T$ are the field profiles of the cavity modes, $\int_d$ denotes spatial integration only over the nonlinear dielectric, and κ_T is a dimensionless constant that quantifies the THz cavity contribution to the nonlinear overlap, defined as:

$$\kappa_T \equiv \sqrt{\frac{\lambda_T^3}{V_{\text{THz}}}} \frac{E_{z,\text{T,NIR}}}{E_{z,\text{T,max}}} \frac{1}{n_{T,\text{max}}}, \tag{2}$$

where $E_{z,\text{T,NIR}}$ is the THz field amplitude inside of the NIR cavity and $E_{z,\text{T,max}}$ is the maximum THz field amplitude, and V_{THz} is the THz mode-volume. Since the TE and TM modes of the dual-mode cavity have near optimal overlap [28], β does not significantly vary with the NIR mode-volumes, but varies with the THz mode volume according to $\beta \sim V_T^{-1/2}$ [24].

Quantum conversion efficiency is quantified by the parameter:

$$E_{\text{ff}}^{\text{Q}} = \frac{\omega_1}{\omega_T \Gamma_1 \Gamma_T} \frac{P_{\text{out,T}}}{P_1}. \tag{3}$$

This parameter describes the number of THz photons collected per photon of signal (ω_1) input that couples into the cavity (factoring in losses). As expected, this parameter is bounded

#115294 - $15.00 USD Received 4 Aug 2009; revised 15 Oct 2009; accepted 19 Oct 2009; published 20 Oct 2009

in the steady state by $E_{\rm ff}^{\rm Q} \leq 1$ [24]. Since the power efficiency ($P_{\rm out,T}/P_1$) is scaled by a factor of $1/\Gamma_1\Gamma_{\rm T}$, a decrease in $\Gamma_1\Gamma_{\rm T}$ causes a decrease in the maximum attainable power efficiency (always occurring at $E_{\rm ff}^{\rm Q} = 1$). Therefore over-coupling of the cavity modes to the corresponding input/output waveguides is imperative for achieving quantum-limited efficiency [24]. As derived in Ref. [24], the efficiency of conversion for any triply resonant DFG system can be expressed as a function only of the input powers, normalized against the critical powers ($P_{1,\rm crit}$, $P_{2,\rm crit}$) defined as,

$$P_{k,\rm crit} \equiv \frac{\omega_k}{16\tilde{Q}\Gamma_k|\beta|^2}\,, \tag{4}$$

where $\tilde{Q} \equiv Q_1Q_2Q_{\rm T}$. This means that only the product of the three Q factors contributes to efficiency and the distribution of this product is unimportant. Figure 2a shows the stable quantum efficiencies reached after a simple continuous-wave (CW) step excitation as a function of normalized input powers. The dotted black line denotes the onset of bistability to its right. Quantum-limited conversion ($E_{\rm ff}^{\rm Q} = 1$) can be achieved when the input powers satisfy $P_2/P_{2,\rm crit} = (1 - P_1/4P_{1,\rm crit})^2$. We can also define a total-efficiency parameter that is proportional to the ratio of THz output power to total input power at both telecom frequencies:

$$E_{\rm ff}^{\rm Tot} \equiv \frac{\omega_1}{\omega_{\rm T}\Gamma_1\Gamma_{\rm T}}\frac{P_{\rm out,T}}{P_1+P_2} = \frac{E_{\rm ff}^{\rm Q}P_1}{P_1+P_2}\,. \tag{5}$$

Quantum efficiency and total efficiency are equivalent in the asymptotic limit, $P_2 \to 0$ ($P_2 \ll P_{2,\rm crit}, P_2 \ll P_1$). In this limit, the conversion efficiency is mono-stable [24]. Total power conversion is optimized when $P_2 \ll P_{2,\rm crit}, P_1 = 4P_{1,\rm crit}$. One can calculate a trajectory in the (P_1,P_2) space that maximizes $E_{\rm ff}^{\rm Tot}$. This corresponds to the optimal operating conditions for a single cavity (fixed $\tilde{Q}$, $\{\omega_k\}$, β) operating through a range of powers. The white dashed curve in Fig. 2a shows the ideal operating conditions for CW THz generation (the limit $\omega_1 \approx \omega_2$). For $P_1 > 4P_{1,\rm crit}$, there do exist solutions with slightly higher efficiency than on this trajectory, but these solutions are only stable for certain Q-factor combinations and cannot be excited with a step CW excitation. Keeping $P_2 << P_1$ for all $P_1 > 4P_{1,\rm crit}$ ensures mono-stable behavior in this region [24].

3. Design

In order to estimate the coupling constant, β, we consider a geometry similar to that shown in Fig. 1: a PhCNC, with closely-spaced TE-like and TM-like modes in the near infrared (NIR) telecom spectral region ($\omega_1/2\pi, \omega 2/2\pi \sim 200$THz) [29] positioned 1 μm above a larger THz cavity. Our cavities, both telecom and THz, are based on a free-standing ridge waveguide patterned with a one-dimensional (1D) lattice of holes, utilizing a tapered photonic-crystal cavity approach that we and others have recently demonstrated [28,30–33]. Each cavity is overcoupled preferentially to the entension of the ridge waveguide at one end (see Fig. 1a) by shortening the cavity's Bragg mirror at that end. We consider the case where both cavities are composed of GaAs ($n_{\rm NIR} \approx 3.45, n_{\rm THz} \approx 3.6$) [7,27]. In addition to its favorable nonlinear properties [7,27], GaAs has low losses in the NIR and mature nanofabrication processes, as evidenced by recent experimental work measuring GaAs photonic-crystal cavities with Q factors as high as 700,000 at 1.55 μm [34–36]. The NIR cavity is suspended slightly above the THz cavity at a height, $d = 1\mu{\rm m} \ll \lambda_{\rm T}$. This particular geometry could be fabricated using sequential lithographic patterning of the NIR and then the THz structures using the appropriate multi-layered wafer. GaAs photonic crystals have also been demonstrated in the THz [37] wavelength region, and THz photonic crystals and photonic crystal cavities have been fabricated in several other materials [38–42]. Practical fabrication of our device would only require that the NIR cavity

#115294 - $15.00 USD Received 4 Aug 2009; revised 15 Oct 2009; accepted 19 Oct 2009; published 20 Oct 2009

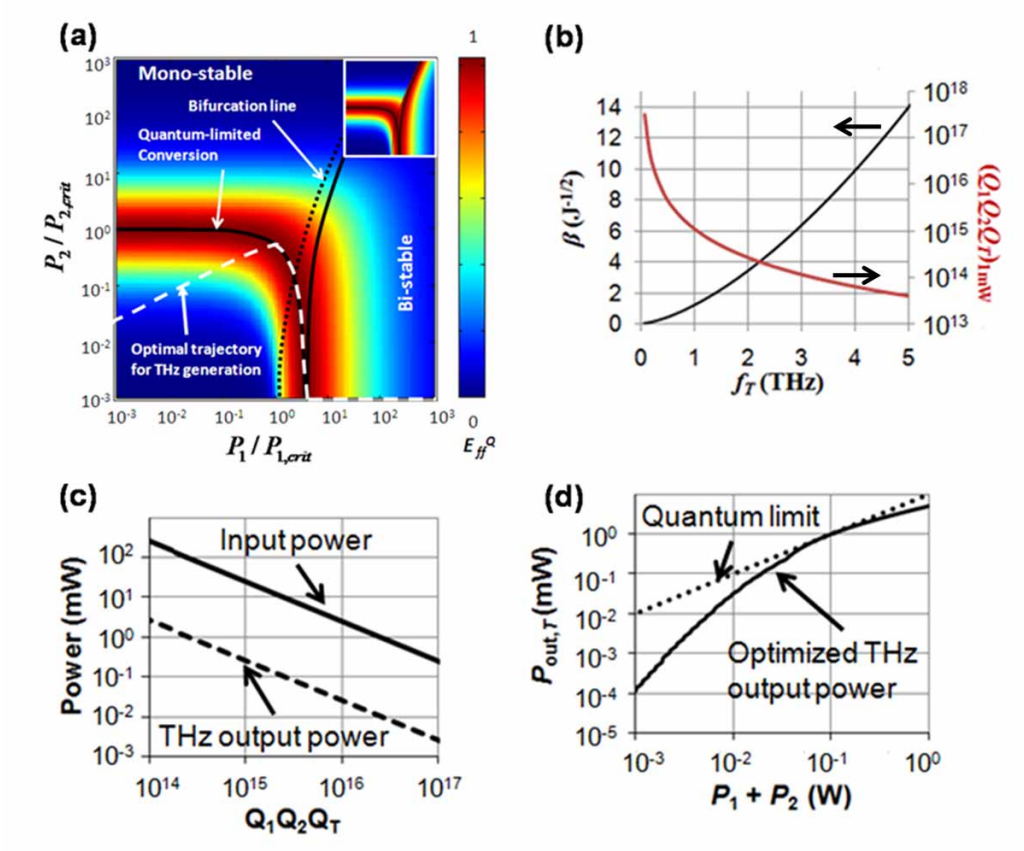

Fig. 2. **(a)** Step-excitable quantum efficiency ($E_{\rm ff}^{\rm Q}$) for stable CW THz generation, plotted as a function of powers of the pump and idler normalized against the critical powers $P_{k,\rm crit}$ (see Eq. (4)). The solid line denotes the critical relationship between input powers where $E_{\rm ff}^{\rm Q} = 1$ is possible ($P_{\rm l} = 4P_{\rm 1,crit}$). The black dotted line denotes the onset of bistability. An inset showing the other stable solution is shown in the top right corner [24]. The white dashed line shows the optimal operating conditions for maximum total conversion efficiency **(b)**: Performance parameters of our nested PhCNC design (GaAs) as a function of the THz resonance frequency: nonlinear overlap, β (left), and the Q-factor product required for 1mW of THz power to be generated from a pump at 200THz with quantum limited efficiency (right). **(c)**: Dependence of the input power (solid line) yielding optimal efficiency ($P_{\rm l} = 4P_{\rm l,crit}$) and the corresponding THz output power (dashed line) on the cavity Q-factor product ($\tilde{Q}$), for coupled GaAs THz and dual mode NIR PhCNCs ($\omega_{\rm l}/2\pi$, $\omega_2/2\pi \sim 200$THz, $\omega_{\rm T}/2\pi \sim 2.0$THz, $\beta \sim 3.5J^{-1/2}$). **(d)**: THz output power as a function of input power in this geometry for, $\tilde{Q} \sim 2.5 \times 10^{14}$. The dotted line shows the quantum limit.

#115294 - $15.00 USD Received 4 Aug 2009; revised 15 Oct 2009; accepted 19 Oct 2009; published 20 Oct 2009

(including input waveguide) be patterned on top of the much larger THz device. The NIR input waveguide could also be coupled to a fiber taper [43].

A 3D finite-difference time-domain code (3D-FDTD) [44] was used to design independent telecom and THz cavities [45], and a CMT model (as described above) was used to describe the nonlinear frequency conversion. We use the design algorithm detailed in Ref. [28] for the design of an NIR PhCNC supporting orthogonal TE-like and TM-like modes, which is necessary to achieve efficient nonlinear conversion as dictated by the $\chi^{(2)}$ tensor of a III–V semiconductor material. We fix the ridge width equal to the regular lattice period (a) and use circular holes in the Bragg-mirror region with radius, $R = 0.3a$. The period and hole radius are then tapered linearly in reciprocal space to 0.84 times the normal value over 8 periods [28]. All cavity dimensions are fixed with respect to the Bragg-mirror lattice period (a) except for the ridge thickness (or height), which is used to tune the frequency spacing between the TE-like and TM-like modes (see Fig. 1d and Ref. [28]). Here we vary the cavity dimensions so that the TE-like resonance is always at 200THz (1.5μm) and the TM-like resonance is at a slightly lower frequency, giving the desired THz difference frequency. The TM-like resonance can also be tuned above the TE-like resonance in frequency, but we find that this gives poorer TM Q factors and lower values of β as the TM-like bandgap shrinks in this direction [28]. The NIR cavity parameters are plotted in Fig. 1c as a function of the desired THz frequency.

For the THz mode, we use a TE-like mode of a large GaAs "nanobeam" cavity (Fig. 1a), having elliptical holes ($R_a = 1.5R_b$) and a four-hole, linear taper of the lattice period and hole diameters. Fig. 1a shows the cavity dimensions as a function of the free-space wavelength of the resonance. The use of elliptical holes for the THz cavity allows us to maximize the area of the mode's fundamental antinode in comparison to the THz wavelength [46]. This cavity can be scaled to fit the desired THz frequency and has $\kappa_T = 0.65$ for any scaling. Moreover, the THz cavity could be replaced by any type of THz cavity having the same value of κ_T, and all operating properties described below would be unchanged. This degree of freedom is a key advantage of our decoupled-design paradigm. The power at which maximum conversion efficiency occurs (normalized $P_1 = 4P_{1,crit}$) for a given THz frequency depends on the product of the three Q factors and the overlap, β. As a numerical example, Fig. 2b shows the dependence on the THz frequency in our design scheme of β and the Q-product required to produce 1mW of THz radiation with optimal efficiency. Figure 2c shows the optimized NIR input power and optimized THz output power as a function of the Q-product for our system for $f_T = 2$THz, $\beta = 3.5\mathrm{J}^{-1/2}$.

Each cavity was first designed to have a Q factor limited by out-of-plane scattering [28, 30]. Overcoupling to the input/output waveguide was then achieved by reducing the length of the Bragg mirror on one side. This reduces the maximum values of the cavity's Q-factor by an order of magnitude, but minimizes the effect of scattering losses by allowing coupling to the waveguide mode be the dominant leakage pathway ($\gamma_{k,s} >> \gamma_{k,l}$) [24, 47], an important requirement for achieving quantum-limited conversion [24]. We find that this tuning of the Bragg mirror lengths has a negligible effect on the overlap β for an order of magnitude variation in the Q-factors. A beneficial consequence of overloading the THz cavity is that the THz output power is then channeled to this waveguide, and thus can be efficiently collected. It is worth noting that GaAs is a low loss material in the THz frequency range [7] and THz generation in GaAs waveguides have been demonstrated experimentally [48].

For some applications where a single cavity must operate across a range of different power levels, the best performance is achieved by varying the two input powers to fit the trajectory described in the previous section (see Fig. 2a). For example, this optimal output power is shown in Fig. 2d for a cavity optimized to produce 1mW of power at 2 THz. This optimization requires a Q-factor product of $\tilde{Q} = 2.5 \times 10^{14}$. When limited by out-of-plane losses, the Q factors of

#115294 - $15.00 USD Received 4 Aug 2009; revised 15 Oct 2009; accepted 19 Oct 2009; published 20 Oct 2009

our TE/TM dual-mode NIR cavity are $Q_1(\mathrm{TE}) = 2 \times 10^7$, $Q_2(\mathrm{TM}) = 3 \times 10^6$ for $f_\mathrm{T} = 2\mathrm{THz}$. Reduction of each mode's Q factor by an order of magnitude to overcouple the waveguide requires a THz Q of only ~ 400. This low requirement is important since realistic THz cavities will be limited by material losses in the THz range. While GaAs has a low absorption coefficient compared to most materials in the THz range, its linear loss rate still corresponds to a Q factor of about 1.5×10^3 [7], which is well below the scattering-limited Q of our design ($Q_{\mathrm{T,scat}} = 1.4 \times 10^6$). THz losses are likely to put an upper bound on any THz cavity Q factor in practice, and further reduction of this limit is then required for overloading to the THz waveguide. As the choice of THz material is unconstrained in our approach, this loss limit can be increased with the discovery of more efficient materials in the THz wavelengths.

The material damage threshold is likely to be the largest obstacle in the operation of such a device and must be considered carefully when implementing this design. Using the coupled-nanobeam design described above, a Q-product of 2.5×10^{14} is optimized such that 1 mW of power is generated at 2THz from 200THz input with quantum-limited efficiency. However, considering a THz cavity in GaAs, with a Q-restricted to $\sim 10^3$, this would require 100 mW of power to be pumped into NIR cavities with Qs on the order of $10^5 - 10^6$, creating a field strength in the cavity that would certainly cause damage. Operating such a device with a 1 mW of NIR input is more realistic, resulting in a reduction of photon conversion efficiency (Fig. 2d), comparable to the current state-of-the-art sources based on DFG in periodically-poled GaAs, but with compact, CW-operation [5]. However our design scheme allows for several modifications that could allow even higher efficiency conversion below the damage threshold. For example, as techniques and materials for confining THz radiation improve, the possibility of making THz cavities with higher-Qs will improve. A value of Q_T only on the order of $\sim 10^4$ (assuming the same value of κ_T would allow 100% photon-conversion of a 1 mW input beam.

A second possible way to overcome damage is to couple many NIR cavities to a single THz cavity. This is possible in our design because the NIR cavity is so small compared to the THz mode profile that many NIR cavities can be fabricated on top of a single THz cavity, all within the fundamental anti-node. For example, in a device producing 2THz of output, a single NIR cavity (including $\sim 5\mu$m long input/output waveguide) covers 370 nm $\times \sim 20$ μm of area out of a total 13 μm $\times$ 56 μm of usable area inside of the fundamental antinode [46]. We can consider an array of N NIR cavities on the anti-node of the THz cavity, as a single NIR cavity. This new effective cavity will have the same Q factor and a N times higher mode volume, but will have the same β/κ_T (see Section 2), yielding an unchanged value of β provided that the array still fits entirely inside a region of the fundamental anti-node with roughly constant THz field amplitude. Thus, this cavity will have the same optimal THz output power, but with a damage threshold that is increased N-fold. However, phase-locking of the inputs to each NIR cavity in the array would be required. This would be the largest challenge in fabricating such an array, but could be overcome for example by coupling each input waveguide to a single source while fixing the relative optical pathlengths in the waveguide-splitter network. Finally, an array of triply-resonant THz devices can be integrated for higher THz output-powers.

4. Conclusion

We have proposed a platform for high efficiency THz generation in triply resonant photonic crystal cavities. By placing a dual-mode photonic-crystal nanobeam cavity with closely spaced TE-like and TM-like resonant modes in the telecom band near the field maximum of a much larger THz cavity mode, we have shown that a high nonlinear overlap of mutually orthogonal modes can be attained in many nonlinear materials (e.g. III–V semiconductors). Total power conversion approaches the quantum limit at a critical power which can be tuned by varying the product of the three mode Q factors. Coupling of many NIR cavities to a single THz cavity

#115294 - $15.00 USD Received 4 Aug 2009; revised 15 Oct 2009; accepted 19 Oct 2009; published 20 Oct 2009

increases the material damage threshold without changing the device performance properties.

Acknowledgements

We would like to thank J.D. Joannopoulos and Marin Soljačić for helpful discussions. IBB and MWM wish to acknowledge NSERC (Canada) for support from PGS and PDF programs. This work is supported through NSEC at Harvard, by the Army Research Office through the ISN under Contract No. W911NF-07-D-0004, and by US DOE Grant No. DE-FG02-97ER25308.

#115294 - $15.00 USD Received 4 Aug 2009; revised 15 Oct 2009; accepted 19 Oct 2009; published 20 Oct 2009